\$ SUPER

Contents lists available at ScienceDirect

Environmental Pollution

journal homepage: www.elsevier.com/locate/envpol





Limited response of boreal forest litterfall mercury deposition to declines in atmospheric mercury concentrations (1987–2000)[★]

Xiangwen Zhang ^{a,b}, Haijun Peng ^{b,c,*}, Stefan Osterwalder ^d, Kevin Bishop ^e, Mats B. Nilsson ^b, Matthias Peichl ^b, Erik Björn ^f, Wei Zhu ^{b,**}

- ^a School of Resources & Environment, Nanchang University, Nanchang, 330031, China
- ^b Department of Forest Ecology and Management, Swedish University of Agricultural Sciences, Umeå, SE-90183, Sweden
- ^c Key Laboratory of Karst Georesources and Environment (Guizhou University), Ministry of Education, College of Resources and Environmental Engineering, Guizhou University, Guiyang, 550025, China
- ^d Department of Geography, Hydrology and Climate, University of Zurich, Zurich, CH-8057, Switzerland
- ^e Department of Aquatic Sciences and Assessment, Swedish University of Agricultural Sciences, Uppsala, SE-75651, Sweden
- f Department of Chemistry, Umeå University, Umeå, SE-90187, Sweden

ARTICLE INFO

Keywords: Litterfall Mercury flux Atmospheric Hg trend Decennial dynamics Seasonal variations Boreal forest

ABSTRACT

Atmospheric mercury (Hg) uptake by vegetation and subsequent deposition via litterfall constitutes a major pathway in the global Hg cycle. However, the temporal dynamics of litterfall Hg deposition and its environmental controls remain poorly understood. Here, we present a detailed assessment of Hg concentrations and deposition fluxes for individual litter components in a Swedish boreal forest from 1987 to 2000. Atmospheric Hg concentrations declined 41 % during this period. Correspondingly, Hg concentrations in Scots pine and Norway spruce needles decreased significantly (\sim 22 % and \sim 26 %, respectively). However, the total litterfall Hg deposition flux remained stable at 11.7 \pm 1.8 µg m $^{-2}$ yr $^{-1}$, showing no clear temporal trend. Foliar litter (needles) contributed 44 % of total Hg deposition, while non-foliar litter (twigs, residual material, and cones) accounted for the remaining 56 % (32 %, 22 %, and 2 %, respectively). The importance of this non-foliar component in modulating litterfall Hg deposition is often overlooked. Litterfall Hg deposition was 1.7 times higher in the non-growing season than in the growing season, primarily due to greater litterfall biomass. The weak response of litterfall Hg deposition to declining atmospheric Hg concentrations highlights the importance of biological factors (e.g., litterfall compositions and productivity) in regulating Hg inputs to boreal forest. Our findings also underscore the need for long-term assessments of Hg deposition dynamics via different litterfall components for assessing the effectiveness of the *Minamata Convention on Mercury*.

1. Introduction

Mercury (Hg) is a pollutant of global concern due to its long-range transport in the atmosphere, high toxicity in the form of methylmercury (MeHg), and strong biomagnification in the food chain (Obrist et al., 2018; Selin, 2009). International efforts, notably the *Minamata Convention on Mercury* — ratified by over 140 countries — aim to reduce Hg emissions and mitigate its environmental impact (Selin and Selin, 2022). Gaseous elemental mercury (Hg⁰, GEM) is the dominant atmospheric Hg species (>95 %), with an atmospheric residence time of

0.3–1.5 years (Horowitz et al., 2017; Obrist et al., 2018). Global Hg emissions are estimated at 6000–8000 Mg yr⁻¹ (Horowitz et al., 2014; Outridge et al., 2018; Selin, 2009; Zhu et al., 2016), with 1000–2400 Mg yr⁻¹ deposited annually in forest ecosystems, representing the largest GEM sink (Wang et al., 2021). Understanding how Hg deposition to forests responds to emission controls and identifying the key factors regulating Hg sequestration in forest ecosystems is critical for assessing the effectiveness of Hg mitigation strategies.

Foliar uptake of GEM through stomata is the primary pathway for Hg sequestration in forests (Arnold et al., 2018; Fu et al., 2016; Liu et al.,

E-mail addresses: hjpeng@gzu.edu.cn (H. Peng), wei.zhu@slu.se (W. Zhu).

https://doi.org/10.1016/j.envpol.2025.126901

Received 20 April 2025; Received in revised form 6 July 2025; Accepted 24 July 2025 Available online 24 July 2025

 $^{^{\,\}star}$ This paper has been recommended for acceptance by Michael Bank.

^{*} Corresponding author. Key Laboratory of Karst Georesources and Environment (Guizhou University), Ministry of Education, College of Resources and Environmental Engineering, Guizhou University, Guiyang, 550025, China.

^{**} Corresponding author.

2021; Obrist et al., 2021; Peckham et al., 2019; Zhou et al., 2021). Litterfall deposition serves as the dominant sink for atmospheric Hg in forest ecosystems, accounting for up to 80 % of total Hg deposition fluxes (Bishop et al., 2020; Jiskra et al., 2015; Wang et al., 2016; Yuan et al., 2023). Litterfall Hg deposition in temperate and tropical forests generally exceeds that in high-latitude coniferous forests, primarily due to greater litterfall biomass production (Navrátil et al., 2019; Wright et al., 2016; Xu et al., 2022; Yuan et al., 2023). Litterfall in tropical and temperate forests is often dominated by broadleaf foliage with relatively lower contributions from woody components (Tang et al., 2010). However, the relative contributions to litterfall Hg deposition by different litterfall components in boreal forests — such as leaves, needles, twigs, bark, and trunk wood — vary significantly due to differences in biomass production and Hg concentrations (Huang et al., 2023; Navrátil et al., 2019; Wright et al., 2016).

Records of Hg accumulation rates in lake sediments (Rydberg et al., 2008), peat deposits (Enrico et al., 2017; Li et al., 2023; Roos-Barraclough et al., 2002), as well as Hg concentrations in ice cores (Fain et al., 2009) and tree rings (Navrátil et al., 2018; Peng et al., 2024) from Europe and North America indicate a decline in atmospheric GEM concentration between 1980 and 2000. In-situ monitoring of atmospheric GEM at Europe's regional background and remote stations suggest a decline from \sim 3.5 ng m⁻³ in 1980s to \sim 1.5 ng m⁻³ in 2000s (Tørseth et al., 2012). This decline was primarily driven by reduced anthropogenic emissions in Europe and North America (Zhang et al., 2016). Forest biomass, including foliage (broad leaves and needles), lichen, and tree rings, has proven to be an effective biomonitor of atmospheric Hg contamination (Assad et al., 2016; Grangeon et al., 2012; Gustin et al., 2022; Matin et al., 2016; McLagan et al., 2022; Peng et al., 2024). Therefore, we expect that reducing anthropogenic Hg emissions will result in a reduction of Hg litterfall deposition in remote ecosystems, benefiting both wildlife and human populations. A pioneering study in North America demonstrated that litterfall Hg deposition in a remote, deciduous tree-dominated mountain forest decreased by approximately 40 % from 2004 to 2015, corresponding to a roughly 25 % decline in atmospheric GEM (Gerson and Driscoll, 2016). In contrast, a recent study examining a quarter-century of Hg concentrations in litterfall from an anthropogenically impacted coniferous forest in central Europe revealed that bark beetle infestations and droughts controlled interannual Hg deposition fluxes (Navrátil et al., 2024). Additionally, an assessment of Hg trends in litterfall from 16 sites in the US Atmospheric Deposition Program revealed no significant changes in litterfall Hg deposition from 2013 to 2021, except at sites influenced by local Hg sources (Gustin et al., 2025). These findings highlight the complex interactions of environmental controls on temporal trends in Hg deposition across different forest ecosystems. To improve our understanding, it is crucial to differentiate the effects of litterfall biomass from Hg concentrations on Hg deposition fluxes, potentially by categorizing specific components of litter that may respond to atmospheric Hg concentrations in distinct ways, particularly in boreal forests.

The boreal forest, predominantly composed of coniferous species such as spruce (e.g., *Picea abies*), pine (e.g., *Pinus sylvestris*), and larch (e.g., *Larix decidua*), is the Earth's second-largest terrestrial biome, covering approximately one-third of the global forest area (Bradshaw and Warkentin, 2015; Gauthier et al., 2015). Previous estimates suggest boreal and temperate forests contribute more than 30 % of the global forest litterfall Hg deposition (Wang et al., 2016). Although Hg deposition on boreal forests is relatively low compared to low-latitude forests, the widespread distribution of boreal forests makes their Hg litterfall deposition of interest. These boreal forests are highly susceptible to climate change and anthropogenic disturbances (Bradshaw and Warkentin, 2015; Gauthier et al., 2015; Vanhala et al., 2016). The boreal forest landscape also contains extensive surface waters, making litterfall Hg deposition a factor in the risk for Hg bioaccumulation in aquatic ecosystems.

Too little is known about how atmospheric Hg deposition to

terrestrial landscapes responds to changes in atmospheric Hg concentrations. This issue is critical to the assessment of the environmental effectiveness of Hg emission control measures, such as those implemented under the *Minamata Convention on Mercury*. In this study, we investigated decadal-scale Hg deposition fluxes via individual litterfall components (needles, twigs, cones and residual unidentified material) in a remote boreal forest in northern Sweden. The objective was to quantitatively assess Hg deposition to boreal forest during a period of rapid atmospheric Hg decline (1987–2000) driven by anthropogenic emission control in Europe. To achieve this, we determined Hg concentrations in individual litterfall components and quantified seasonal to decadal litterfall Hg deposition fluxes over that 14-year period. Our findings contribute to the pressing need for knowledge to assess the global environmental effectiveness of the *Minamata Convention on Mercury*.

2. Materials and methods

2.1. Site descriptions

Seasonal litterfall sampling was conducted at the Svartberget Experimental Forest (SVB, 64°14′N, 19°46′E, average elevation 267 m a. sl., Fig. 1a and b), approximately 70 km northwest of Umeå, northern Sweden (Laudon et al., 2013; Lee et al., 2000). The climate at SVB is classified as cold temperate humid, with a 30-year (1986-2015) mean annual precipitation of 619 mm and an average air temperature of 2.1 °C. The bedrock in the Krycklan catchment is predominantly composed of Svecofennian metasediments/metagraywacke (~94 %), with minor contributions from acidic and intermediate metavolcanic $(\sim 4\%)$ and basic metavolcanic $(\sim 3\%)$ rocks. The soils primarily consist of Quaternary deposits, dominated by till (~51 %) and sorted sediments $(\sim 30 \%)$. The growing season at SVB typically extends from early May to late October, with the remainder of the year characterized by frozen conditions and snow cover. In this study, we define the growing season as May to October and the non-growing season as November to April. The SVB spans approximately 1520 ha and is primarily composed of coniferous species, with Scots pine (Pinus sylvestris) and Norway spruce (*Picea abies*) accounting for \sim 63 % and \sim 26 % of the forest, respectively. The remaining ~11 % consists of deciduous species, including birch Betula spp. (Chi et al., 2020; Peichl et al., 2023). The average tree height at SVB is 19 m. Although needles are shed seasonally by pine and spruce canopies, pine trees generally retain their needles for 2–3 years, whereas spruce trees can retain them for 3-7 years (Reich et al., 1996).

2.2. Sample collection

Twenty-eight rectangular litterfall traps (0.5 \times 0.5 m, 60 cm above ground) were randomly deployed across the SVB, where the dominant tree stands are approximately 130 years old in the 2000s (Peichl et al., 2023). The forest consists of two distinct topographic regions: hillslopes dominated by Scots pine (Pinus sylvestris) and lowlands dominated by Norway spruce (Picea abies). To account for the relative land cover of each species, litter traps were placed in spruce-dominated stands (18 traps) and pine-dominated stands (10 traps), with the two stands located nearby (within 1 km) of each other. From 1987 to 2000, the litter was collected biannually in May (after snowmelt) and October (before freezing), representing non-growing and growing season samples, respectively. During the non-growing seasons of 1987 and 1988, one and seven traps, respectively, were damaged due to heavy snow. Litterfall biomass production for these seasons was estimated without data from the affected traps, and new traps were subsequently installed at the same locations to maintain continuous sampling. Collected litter samples were dried immediately at 65 °C in the laboratory (~24-48 h) (Wohlgemuth et al., 2020) and sorted into seven categories: pine needles (PN), spruce needles (SN), pine twigs (PT), spruce twigs (ST), pine cones (PC), spruce cones (SC), and residual unidentified fragments (including lichens, bark, flower buds, bud scales, deciduous leaves, insects, conifer seeds, etc.).

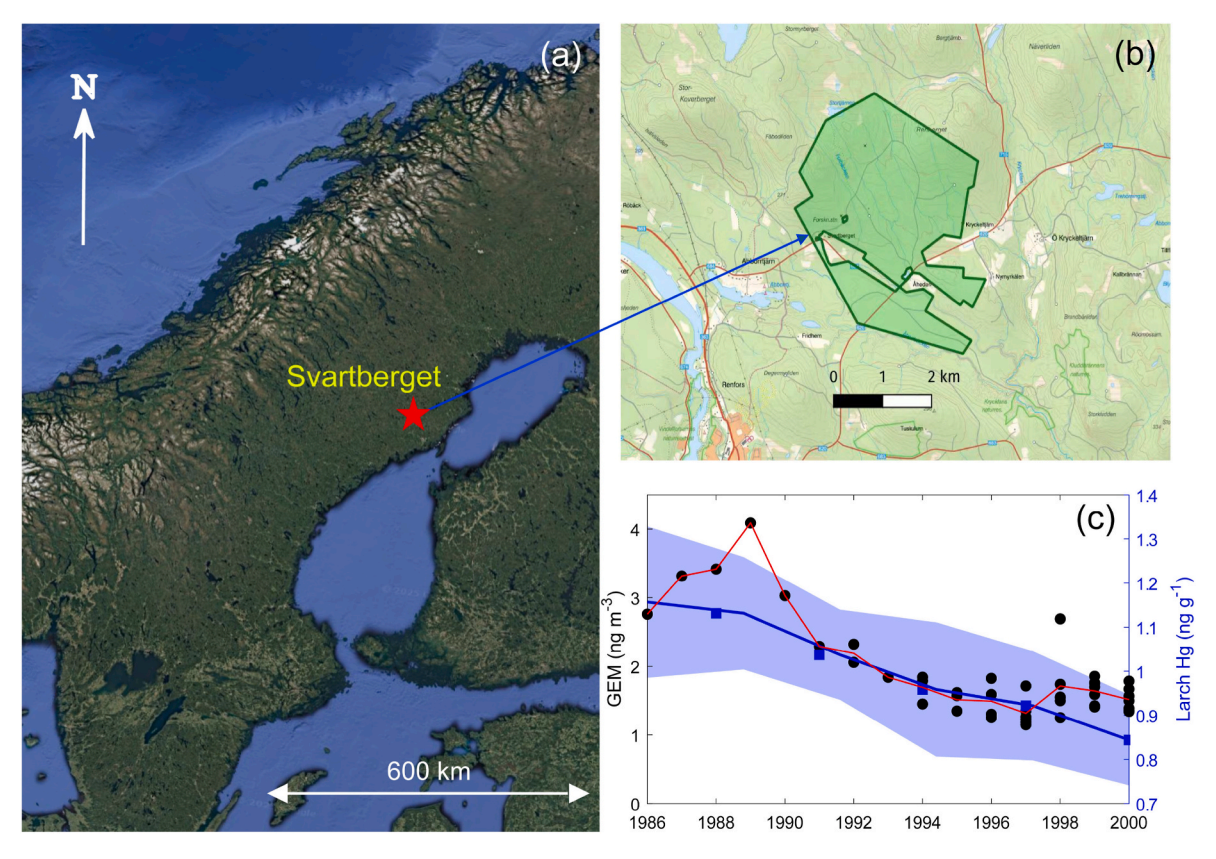


Fig. 1. (a) Map showing the location of Svartberget Experimental Forest (SVB) in northern Sweden. (b) Zoomed in map of the SVB site (green line edge), note the background map is from Lantmäteriet. (c) annual-average atmospheric GEM concentration at background sites across Europe (black circle points and red line) and larch tree-ring Hg concentrations at SVB (blue rectangular points and blue line) (Enrico et al., 2017; Peng et al., 2024; Tørseth et al., 2012). (For interpretation of the references to colour in this figure legend, the reader is referred to the Web version of this article.)

This latter category is hereafter referred to as "other-material". The dried samples from each category, collected within the same season and year, were homogenized before determining their respective weights for biomass estimation. Three aliquots (\sim 3–5 g each) were taken from the homogenized samples and finely milled (IKA Tube Mill) for subsequent chemical analysis.

2.3. Hg analysis and ancillary measurements

Total Hg concentrations in all litterfall fractions were determined using a Direct Mercury Analyzer (DMA-80 Tricell, Milestone Srl, Italy). Each sample was analyzed in duplicate, with variations typically remaining below 10 %. If the variation between replicates exceeded 10 %, a third measurement was performed. Samples were weighed and placed in clean nickel boats for analysis. Prior to use, nickel boats were cleaned and combusted in a muffle furnace at 550 °C for 2 h. For quality control, daily measurements began with three blanks (empty nickel boats) followed by three measurements of a certified reference material (apple leaves, NIST 1515). The recovery of NIST 1515 remained consistently within 90–110 %. During sample analysis, a primary certified reference material (pine needles, NIST 1575a) and a blank were analyzed every 10 measurements. The measured Hg concentration of the NIST 1575a was 39.1 \pm 0.3 ng g⁻¹ (\pm SD, n = 92), closely matching the certified value of 39.9 \pm 0.7 ng g⁻¹, confirming the accuracy of total Hg recovery in biomass samples (Peng et al., 2024). A total of 266 samples were analyzed for Hg concentrations, including 46 SN, 36 PN, 38 SC, 34 PC, 38 ST, 36 PT, and 38 samples of other-material. Hg deposition flux in litterfall (i, representing a specific litter component or the total) was calculated by integrating Hg concentrations (µg kg⁻¹) with biomass production (kg m^{-2} yr⁻¹).

$$Hg \ deposition_i = \sum_i Hg \ concentration_i \times biomass_i$$
 (1)

Meteorological data were obtained from the SVB reference climate monitoring station (225 m a.s.l.) (Laudon et al., 2013; Noumonvi et al., 2023). In brief, air temperature was measured at 1.7 m above ground using a sensor housed in a ventilated radiation shield. Precipitation was measured manually using a standard SMHI gauge positioned at 1.3 m above ground. Wind speed was measured with a RM Young propeller anemometer installed at a height of 38 m. Annual mean atmospheric GEM concentrations at background sites across Europe (Fig. 1c) were obtained from the European Monitoring and Evaluation Program (EMEP) (Tørseth et al., 2012) and have been reported in previous studies (Enrico et al., 2017; Peng et al., 2024).

2.4. Statistical methods

All statistical analyses were conducted using MATLAB software (R2020b, The MathWorks, Inc.). A paired-sample t-test (the 'ttest' function in MATLAB) was performed to assess whether Hg concentrations and deposition fluxes differed significantly (p < 0.05) between the growing and non-growing seasons. Principal component analysis (PCA) was conducted using the 'pca' function in MATLAB, with all data normalized via the 'zscore' function prior to analysis. Correlation coefficients between different data groups, along with their corresponding p-values, were computed using the 'corrcoef' function."

3. Results and discussions

3.1. Hg concentrations in litterfall components

The Hg concentrations in litterfall components of Norway spruce were generally higher than those of Scots pine (Fig. 2a). Among all litterfall components, twigs exhibited the highest Hg concentrations, while cones showed the lowest. Specifically, Hg concentrations in spruce twigs (ST) ranged from 172.0 to 244.8 $\mu g~kg^{-1}$, with a mean of 204.9 \pm 20.6 $\mu g \ kg^{-1}$ (mean \pm 1SD, dry weight), making them the component with the highest Hg concentration. The mean Hg concentrations in other litterfall components were 106.4 \pm 32.9 $\mu g~kg^{-1}$ for pine twigs (PT), 62.8 \pm 7.9 $\mu g~kg^{-1}$ for spruce needles (SN), 38.3 \pm 5.1 $\mu g~kg^{-1}$ for pine needles (PN), $23.7 \pm 7.0 \ \mu g \ kg^{-1}$ for spruce cones (SC), and 13.6 ± 9.4 μg kg⁻¹ for pine cones (PC). The non-growing season residual material in litterfall (categorized as "other-material", Fig. 2a) showed the greatest variability in Hg concentration, ranging from 43.4 to 214.6 μg kg⁻¹, with a mean of 130.5 \pm 49.5 $\mu g\,kg^{-1}.$ No significant seasonal differences in mean Hg concentrations were observed for needles, cones, or twigs. However, the mean Hg concentration in the "other-material" category was significantly higher during the non-growing season compared to the growing season (130.5 \pm 49.5 μ g kg $^{-1}$ vs. 103.3 \pm 38.7 μ g kg $^{-1}$, *t*-test, *p*

The substantial variation in Hg concentrations among litter components in the SVB boreal forest (Figs. 2a and 3) aligns with findings from subalpine and temperate coniferous forests (Huang et al., 2023; Navrátil et al., 2019). The markedly higher Hg concentrations in twigs and other-material compared to needles and cones may result from the translocation and assimilation of Hg, as well as the physiological and biological stabilization of Hg compounds in plant tissues. Mercury enters the tree mainly through stomatal GEM uptake (Gustin et al., 2022; Peckham et al., 2019; Wang et al., 2021; Yuan et al., 2023), whereas the translocation of the Hg accumulated from foliar to other tree tissues and their subsequent stabilization remains to be constrained. Our results show that twigs and other-material litter have substantially higher Hg concentrations than needles and cones (Fig. 2a), suggesting a greater capacity for Hg assimilation in the former. Since trunk wood Hg concentration (mean = \sim 1.5 ng g⁻¹) (Peng et al., 2024) is substantially lower than that in needles and bark by 1-2 orders of magnitudes (Navrátil et al., 2019; Yang et al., 2018), the higher Hg concentration in twigs and other-material litter are largely due to the elevated Hg content in bark and lichen material. Similarly, lichen has been identified as a

primary contributor to Hg deposition in a Swiss subalpine forest (Huang et al., 2023).

On regional spatial scales, the spruce needle Hg concentrations from the northern Sweden forest (62.8 $\mu g \ kg^{-1}$) were lower than those in temperate spruce forests in the Czech Republic (79–97 µg kg⁻¹) (Navrátil et al., 2019; Navrátil et al., 2025) but higher than those in an alpine spruce forest in Switzerland (49.9 μg kg⁻¹) (Huang et al., 2023). This pattern broadly aligns with the atmospheric Hg concentrations at the respective sites (Chen et al., 2023; Peng et al., 2024). Needle Hg concentrations in the remote northern Swedish boreal forest are similar to the global average litterfall Hg concentration (54 µg kg⁻¹) (Wang et al., 2016) and the nationwide mean litterfall reported for China (52.0 μg kg⁻¹) (Xu et al., 2022), but slightly higher than those in the eastern USA (40.6 μ g kg⁻¹) (Risch et al., 2017). However, it should be noted that these comparisons are based on reported mean values, and substantial variability may exist within litterfall samples from each region. Additionally, differences in species composition, canopy structure, and the age distribution of litterfall from various regions can contribute to variability in Hg concentrations. Foliar Hg concentration increases throughout the growing season (Siwik et al., 2009) and continues to accumulate over multiple seasons in evergreen coniferous needles, such as spruce and pine needles (Wohlgemuth et al., 2020). On seasonal timescales, our results showed no significant difference in mean Hg concentrations between the growing and non-growing seasons in needles, cones, and twigs (Fig. 2a), suggesting minimal or slow Hg uptake during the non-growing season. This, however, may be obscured by interannual and among-sample variability. In addition, GEM can also be assimilated by trees through non-stomatal pathways, such as surface adsorption via e.g., bark, foliage and twigs (Chiarantini et al., 2016; Stamenkovic and Gustin, 2009). Due to the longer residence time of non-foliar litter components - such as twigs, which may remain on trees for up to several decades - compared to needles (typically less than five years) and cones (Muukkonen and Lehtonen, 2004), the substantially higher Hg concentrations in twigs and other-material are largely attributed to prolonged surface adsorption from the atmosphere. Additionally, tree species composition plays a crucial role in Hg deposition, influencing the Hg concentrations of individual litterfall components (Barquero et al., 2019; Wohlgemuth et al., 2022). In this study, litterfall (needles, cones, and twigs) from spruce trees exhibited significantly higher Hg concentrations than those from pine trees (Fig. 2a), suggesting a greater Hg assimilation capacity in spruce.

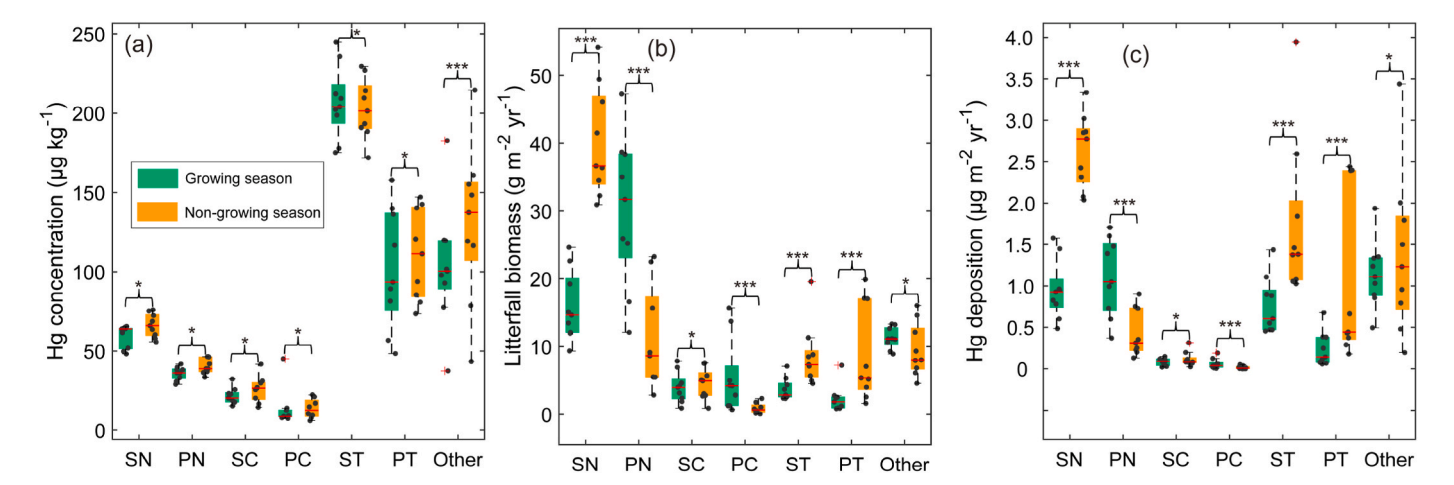


Fig. 2. Boxplots of (a) litterfall Hg concentrations, (b) litterfall biomass, and (C) litterfall Hg deposition flux of all individual components [spruce needles (SN), pine needles (PN), spruce cones (SC), pine cones (PC), spruce twigs (ST), pine twigs (PT), and other residual unidentified material (other)] during the growing season (green) and non-growing season (orange). The box boundaries represent the 25th and 75th percentiles and the red solid horizontal line in the box represents the median value. Black cross hatches indicate the 5th and 95th percentiles. The black solid dots are the individual measurements, and the red cross denotes the outlier. The symbols *** denote significant difference of mean values between two groups (t-test, p < 0.05), while * denotes they are insignificance differences (t-test, p > 0.05). (For interpretation of the references to colour in this figure legend, the reader is referred to the Web version of this article.)

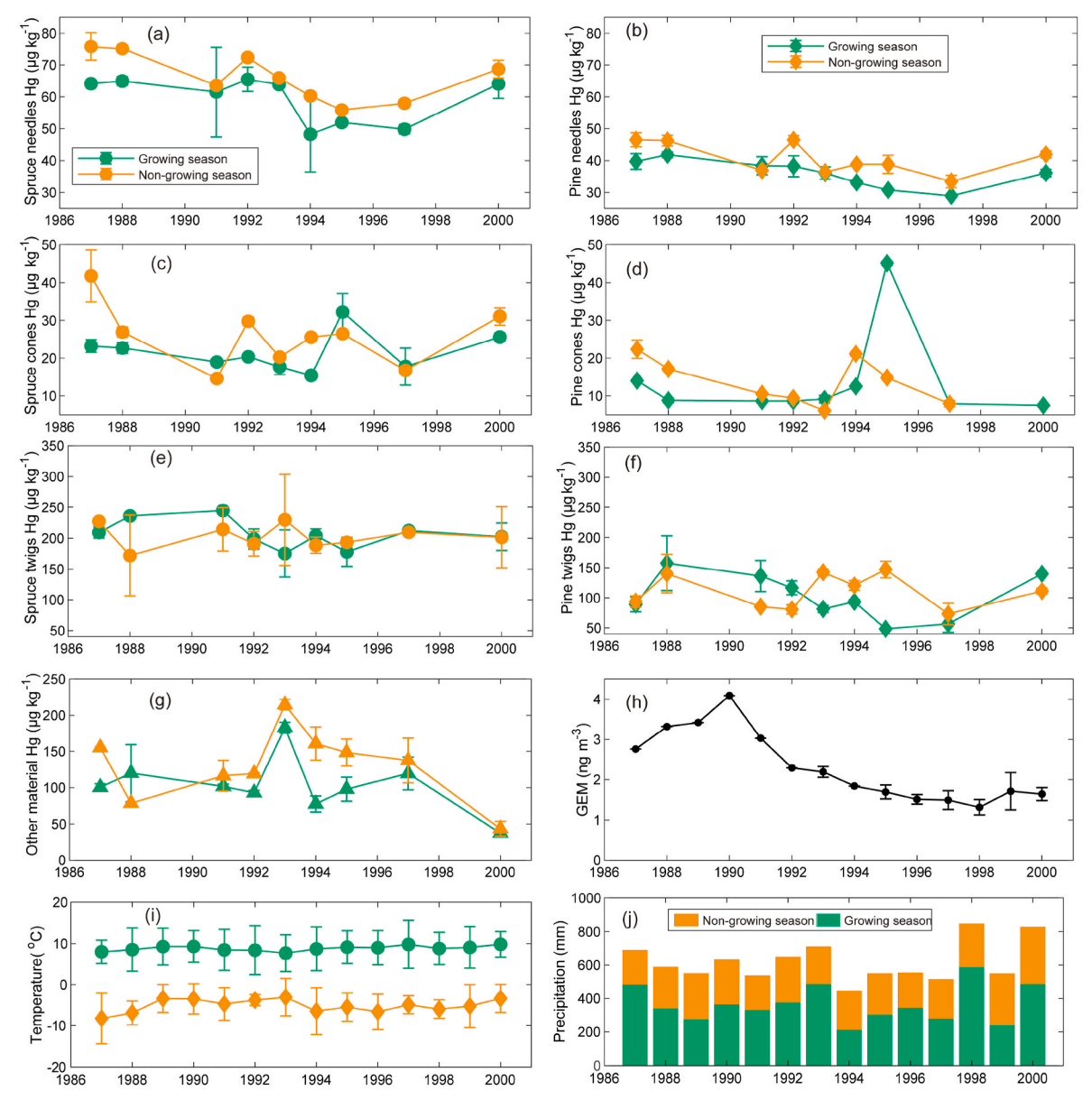


Fig. 3. Time series of individual litterfall components' Hg concentrations (a–g), atmospheric GEM concentrations (h), air temperature (i), and precipitation (j). Error bars represent ±1SD.

3.2. Litterfall biomass and Hg deposition

The total mean annual litter biomass deposition from 1987 to 2000 was 156 \pm 19.6 g m $^{-2}$ yr $^{-1}$, with the highest and lowest litterfall biomass of 131 (1991) and 181 (1997) g m $^{-2}$ yr $^{-1}$, respectively (Fig. 2b). The relative contribution of needles, twigs, cones, and othermaterial fractions to total litter biomass was 62.1 \pm 5.4 %, 15.0 \pm 5.4 %, 9.3 \pm 3.7 %, and 13.5 \pm 3.1 %, respectively. In contrast to the similarity of Hg concentrations in litterfall components (needles, cones, and twigs) between growing and non-growing seasons (Fig. 2a), litterfall biomass deposition showed significant seasonal differences (Fig. 2b).

During the fourteen years of this study, 1987-2000, the average annual litterfall Hg deposition flux was $11.7 \pm 1.8 \,\mu g \,m^{-2} \,yr^{-1}$ ($\pm 1SD$, Fig. 4). Seasonal patterns of litterfall Hg deposition showed significantly lower fluxes in SN, ST, and PT during the growing season compared to the non-growing season, whereas PN and PC exhibited higher fluxes during the growing season (Figs. 2c and 4). This characteristic seasonal trend aligns with the biomass production of respective litterfall components (Fig. 2b), emphasizing the role of biomass production in

regulating litterfall Hg deposition in the boreal forest. Our observed litterfall Hg deposition flux in the northern Swedish boreal forest (11.7 \pm 1.8 μg m $^{-2}$ yr $^{-1}$) is similar to that in deciduous, mixed, and coniferous forests of the eastern USA (median = 11.7 μg m $^{-2}$ yr $^{-1}$, range: 2.2–23.4 μg m $^{-2}$ yr $^{-1}$) (Risch et al., 2017; Zhou et al., 2023). However, this flux is on the lower end of global forests litterfall Hg deposition (median = 15.3 μg m $^{-2}$ yr $^{-1}$, range: 2.7–220 μg m $^{-2}$ yr $^{-1}$, n = 90) (Wang et al., 2016), accounting for only half of the national average in China (25.9 \pm 12.5 μg m $^{-2}$ yr $^{-1}$) (Xu et al., 2022), and substantially lower than values reported for forests in central Europe (23–73 μg m $^{-2}$ yr $^{-1}$) (Huang et al., 2023; Navrátil et al., 2025).

In contrast to the dominance of foliar biomass in litterfall Hg deposition in deciduous and evergreen forests (Wang et al., 2021), coniferous forest litterfall composition is more diverse, with substantial contributions from non-foliar biomass. At SVB, foliar (needles) and non-foliar (twigs, cones, and other-material) litter accounted for 62 % and 38 % of the total biomass, respectively (Fig. 2a). However, Hg deposition flux from needles (44 %) was lower than that from non-foliar components (56 %), driven by the significantly higher Hg concentrations in twigs and

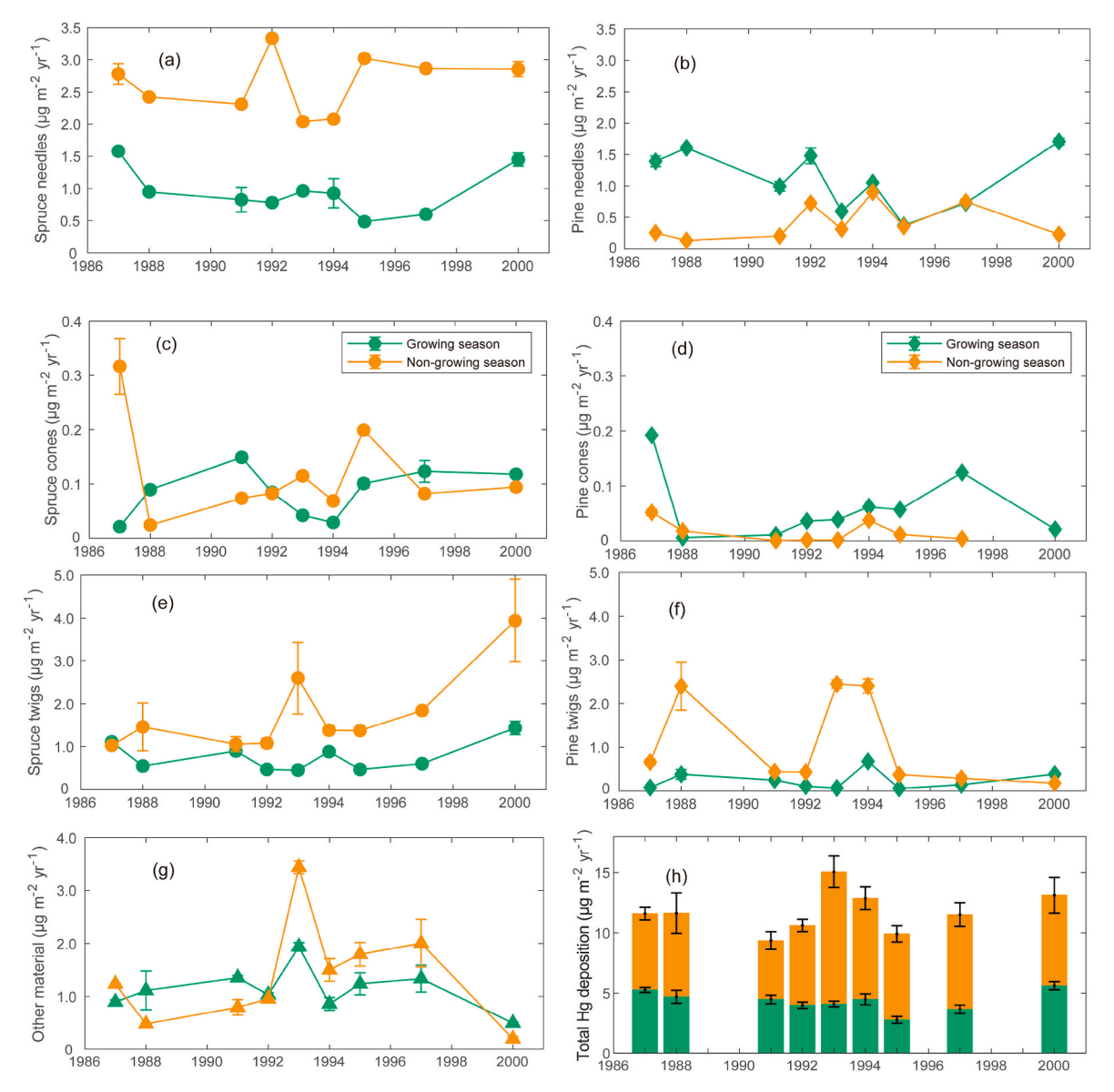


Fig. 4. Temporal evolution of growing season (green) and non-growing season (orange) litterfall Hg deposition flux: individual litterfall components (a–g), and total litterfall deposition flux (h). Error bars represent \pm 1SD. (For interpretation of the references to colour in this figure legend, the reader is referred to the Web version of this article.)

other-material litter (Fig. 2c). Litterfall components, needles, twigs, cones, and other-material, on average contributed 5.1 \pm 0.8, 3.8 \pm 1.5, $0.3\pm0.1,$ and $2.5\pm1.2\,\mu g\,m^{-2}\,yr^{-1}\,Hg$ deposition flux, which accounts for 44 \pm 8.7 %, 32 \pm 9.0 %, 2 \pm 1.2 %, and 22 \pm 8.8 % of the total flux, respectively. Similar diverse patterns of litterfall Hg deposition have been observed in other coniferous forests (Huang et al., 2023; Navrátil et al., 2019). The contribution of needles and cones to annual Hg deposition at SVB aligns with findings from temperate spruce forests in the central Europe, where needles and cones account for 45.5 \pm 3.5 % and 3.5 \pm 0.5 % of total deposition, respectively (Navrátil et al., 2019). Similar patterns were observed in an alpine spruce forest in central Europe, with contributions of 40 \pm 2.2 % (needles) and 4.0 \pm 0.3 % (cones) (Huang et al., 2023). In contrast, twigs contributed only 16 \pm 2.5 % to total litterfall Hg deposition in the alpine spruce forest. Notably. lichen and other fine litter accounted for 40.0 \pm 1.4 % in the alpine spruce forest, substantially higher than in temperate spruce forest (5 \pm 2%) and the other-material category in the boreal forest of our study (22 \pm 8.8 %). The large site-specific differences in the contribution of various litterfall components to total Hg deposition in coniferous forests

are driven by the combined effects of climate-related litter production and the Hg uptake capacity of each component. Our findings highlight the importance of carefully categorizing individual litter components to ensure high-quality forest Hg deposition datasets, given the substantial spatial and temporal variations in Hg concentrations and biomass productivity.

A previous study on foliar Hg uptake during the 2018 growing season modelled an average uptake rate of $11\pm1~\mu g$ Hg m $^{-2}$ and $4\pm1~\mu g$ m $^{-2}$ for spruce and pine trees for ten sites across Europe, and a lower uptake of 7.1 \pm 3.8 μg Hg m $^{-2}$ and 4.9 \pm 0.9 μg m $^{-2}$ for spruce and pine trees for SVB site (Wohlgemuth et al., 2020). However, our litterfall measurements indicate that the decadal average (1987–2000) annual Hg deposition flux was $3.6\pm0.5~\mu g$ Hg m $^{-2}$ yr $^{-1}$ for spruce needles and 1.5 \pm 0.5 μg Hg m $^{-2}$ yr $^{-1}$ for pine needles at SVB site in this study. The discrepancy between our observed needle Hg deposition flux (1987–2000) and model estimates for 2018 may stem from uncertainties in biomass productivity estimates and interannual variability. In temperate and alpine spruce forests of central Europe, elevated Hg deposition fluxes of 15–34 μg Hg m $^{-2}$ yr $^{-1}$ (Navrátil et al., 2019;

Navrátil et al., 2025) and 10 μg Hg m $^{-2}$ yr $^{-1}$ (Huang et al., 2023) have been observed in spruce needles. Coniferous trees growing in the colder high latitude regions have longer needle life span (Reich et al., 2014), which may prolong the GEM uptake by needles in boreal forest. Given that needle Hg concentrations in these forests varied by less than a factor of two (50–97 μg kg $^{-1}$, Section 3.1), the 3–10 times higher needle Hg deposition flux (3.6 vs. 10–34 μg Hg m $^{-2}$ yr $^{-1}$ in boreal and central Europe, respectively) is primarily driven by enhanced needle biomass production in central European forests.

3.3. Temporal trends and drivers of litterfall Hg concentrations

Peng et al. (2024) reconstructed historical atmospheric GEM at SVB using tree-ring archives (three years intervals) and *in-situ* atmospheric monitoring. Combined with previous studies on peat archives and varved lake sediments from nearby sites (Li et al., 2023; Rydberg et al., 2008), these results indicate a steep decline in atmospheric GEM at SVB from the 1970s to the 2000s. Between 1987 and 2000, larch tree-ring Hg concentrations decreased by 35 %, from 1.16 μ g kg $^{-1}$ to 0.82 μ g kg $^{-1}$ (Fig. 1c), corresponding to a 41 % decline in atmospheric GEM, from 2.7 ng m $^{-3}$ to 1.6 ng m $^{-3}$ (Peng et al., 2024). This trend closely aligns with compiled atmospheric GEM concentrations at remote sites across Europe (Fig. 1c), as reported by EMEP (Tørseth et al., 2012). Therefore, we adopt the annual average atmospheric GEM concentrations from European remote sites (Figs. 1c and 3h) for factor analysis to disentangle the

drivers of temporal trends in litterfall Hg concentrations (Section 3.3) and deposition fluxes (Section 3.4).

Temporally, pine needle Hg concentrations exhibited a significant decreasing trend ($r^2 = 0.51$, p < 0.05, Fig. 3b and Fig. S1), with a decline rate of 0.7 μ g kg⁻¹ yr⁻¹, resulting in an overall reduction of ~22 % during the period of 1987–2000. In contrast, the decline in spruce needle Hg concentrations was weaker and statistically insignificant when all data were included ($r^2 = 0.28$, p = 0.14), primarily due to an abrupt increase in the year 2000. When excluding the year 2000 data, the spruce needle Hg concentration exhibited a significant decline (r^2 = 0.75, p < 0.01, Fig. 3a and Fig. S1) at a rate of 1.9 μ g kg⁻¹ yr⁻¹, with a total decrease of ~26 % from 1987 to 1997. However, this exclusion should be interpreted with caution. The elevated spruce needle Hg concentration in the year 2000 may reflect anomalous conditions, such as variation in needle retention time or a biological pulse year, rather than a reversal of the long-term trend. Despite this variability, the observed decline over the 13 year period prior to 2000 (1987–1999) is consistent with decreasing atmospheric Hg concentrations. This response is further supported by significant correlations between atmospheric GEM concentrations and Hg levels in both spruce and pine needles (Fig. S2). Given that the needles are growing for multiple years, the determined litterfall needle Hg concentrations are not fully independent for each specific year. This is evidenced by autocorrelation analysis of spruce and pine needle Hg concentrations time-series data, which yielded a Durbin-Watson statistic <2. While this does not negate

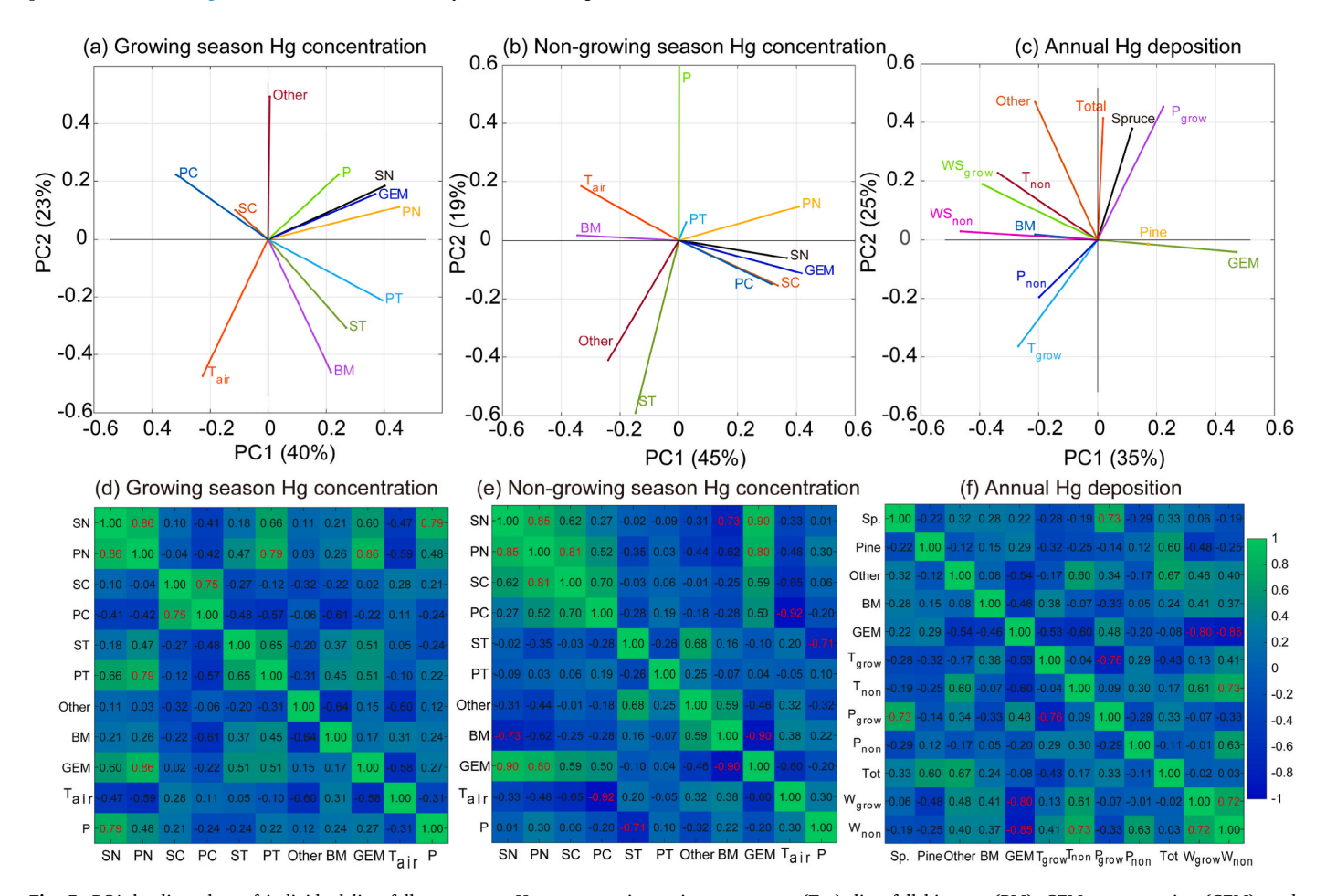


Fig. 5. PCA loading plots of individual litterfall component Hg concentrations, air temperature (T_{air}), litterfall biomass (BM), GEM concentration (GEM), and precipitation amount (P) during the growing season (a) and non-growing season (b). PCA loading plot (c) of annual total (Tot), Spruce (Sp.), Pine, and other-material litterfall Hg deposition; growing season air temperature (T_{grow}), precipitation (P_{grow}), wind speed (W_{grow}); and non-growing season air temperature (T_{non}), precipitation (P_{non}), wind speed (W_{non}). Pearson correlation matrix of the growing season (d) and non-growing season (e) litterfall Hg concentrations, and (f) annual total Hg deposition with environmental variables. Values in the correlation matrix are the correlation coefficients (r) with red fonts showing significant correlations (p < 0.05). (For interpretation of the references to colour in this figure legend, the reader is referred to the Web version of this article.)

the observed declining trend, it idicates that the linear regression may underestimate the associated uncertainty. Future work using expanded datasets and time series regression models could better quantify trend significance under autocorrelated conditions. Nevertheless, these results suggest that spruce and pine needles reliably captured the decadal decline in atmospheric GEM concentration (41 %), supporting previous findings that conifer needles are good biomonitors of changes in atmospheric Hg concentrations (Navrátil et al., 2019; Navrátil et al., 2024).

In contrast to the 41 % decline in atmospheric GEM concentrations and the significant reductions in Hg concentrations of spruce and pine needles (~22 % and ~26 %, respectively) between 1987 and 2000, linear regression analysis revealed no statistically significant temporal trends (p > 0.05) in total Hg concentrations for cones, twigs and othermaterial litter components during either growing or non-growing seasons (Fig. 3c-g). Principle component analysis (PCA, Fig. 5a-b, d-e, Tables S1–S2) assessing the relationships between Hg concentrations in litterfall components and environmental variables, including atmospheric GEM concentrations (Fig. 3h), air temperature (Fig. 3i), precipitation (Fig. 3j), and litterfall biomass, indicated a positive but statistically insignificant (p > 0.05) correlation between atmospheric GEM concentrations and Hg concentrations in growing season twigs and non-growing season cones. The weaker influence of atmospheric GEM on Hg concentrations in non-foliar litter (twigs, cones, and othermaterial components) may be related to the following factors: (1) nonfoliar litter, such as twigs, bark and lichen, has a longer residence time - up to decades - providing prolonged opportunities for Hg accumulation, which may obscure the effects of changing atmospheric Hg levels on a decadal scale. (2) The mechanisms governing Hg accumulation in non-foliar litter are more complex than those in needles, involving in vivo Hg transport following atmospheric uptake by foliage. Interestingly, precipitation was positively correlated with growing season needle Hg concentrations (Fig. 5d) but showed no association with non-foliar litter. This may be explained by the stimulation of needle stomatal conductance by increased precipitation, which in turn facilitates stomatal GEM uptake (Blackwell et al., 2014; Méndez-López et al., 2023; Wohlgemuth et al., 2020).

3.4. Temporal trends and drivers of litterfall Hg deposition

From 1987 to 2000, litterfall Hg deposition flux remained constant (mean = $11.7 \pm 1.8 \ \mu g \ m^{-2} \ yr^{-1}, \pm 18D$) with no significant temporal trend ($r^2 = 0.05, p = 0.55$, Fig. 4h and Fig. S3) at SVB, ranging between 9.4 $\mu g \ m^{-2} \ yr^{-1}$ (1991) and 15.1 $\mu g \ m^{-2} \ yr^{-1}$ (1993), despite a gradual ~41 % decline in atmospheric GEM (Section 3.3). Despite missing data for five individual years spread among the 14 years covered in the study, the available measurements still span the full period. PCA and correlation analyses of annual total litterfall Hg deposition flux against relevant biological (total biomass deposition, spruce and pine litterfall Hg deposition flux) and environmental variables (atmospheric GEM, temperature, precipitation, and wind speed) revealed no statistically significant relationships for any examined factor (p > 0.05, Fig. 5c and f, Table S3). Although atmospheric GEM is the predominant source of Hg in aboveground biomass (Wang et al., 2021), the PCA results suggest that no single factor can be identified as the primary control on litterfall Hg deposition in boreal forests.

Temporal trend analyses were conducted for the deposition flux of all litter components (needles, cones, twigs and other-material, Fig. 4a–g), revealing no significant trends (p>0.05, regression not shown). The contrasting temporal patterns of Hg concentrations in spruce and pine needles (i.e., significant declines) versus Hg deposition fluxes (i.e., no significant trends) underscore the critical role of needle biomass deposition flux in modulating the temporal trends of Hg deposition flux. Correlations between litterfall component Hg deposition flux and respective Hg concentrations (Fig. S4) or litterfall biomass (Fig. S5) indicate that Hg deposition within each litterfall component is primarily governed by its biomass deposition. This is further confirmed by

performing partial correlation analysis of litterfall component Hg deposition flux versus biomass through controlling the variable litterfall Hg concentrations (p < 0.05, not shown). Our finding aligns with observations from deciduous and mixed forests in eastern USA (Gustin et al., 2025; Risch et al., 2017). However, total litterfall biomass deposition flux and the biomass deposition flux of individual components exhibited no significant temporal trends over the decadal study period (Fig. S6). Although total needle biomass accounted for ~62 % of total litterfall biomass and its Hg concentration declined by 22.4 %-26.1 %, the moderate interannual variability of total needles biomass (ranging from 71.2 to 117 g m⁻² yr⁻¹, with a coefficient of variance of 16.6 %, Fig. S6) resulted in no significant trend in total needle Hg deposition flux. Additionally, regression analyses of total litterfall Hg deposition flux against foliar (needle) Hg deposition flux (Fig. S7a) and non-foliar (cones, twigs, and other-material) Hg deposition flux (Fig. S7b) demonstrate that non-foliar litterfall Hg deposition flux (ranging from 4.3 to 11.1 μ g m⁻² yr⁻¹, with a coefficient of variance of 30.2 %) explains 80 % of the interannual variability in total litterfall Hg deposition flux. These results highlight the vital role of non-foliar litterfall in regulating the temporal trends of Hg deposition, as Hg concentrations in non-foliar litter components are less responsive to atmospheric GEM concentrations changes. The relatively stable litterfall Hg deposition flux (mean = $11.7 \pm 1.8 \ \mu g \ m^{-2} \ yr^{-1}, \pm 1SD$) at our boreal forest site can be attributed to two key factors: (1) the effect of declining needle Hg concentrations on needle Hg deposition flux was offset by the moderate interannual variability of needle biomass deposition, (2) non-foliar litterfall Hg deposition flux, which constituted 56 % of the total litterfall Hg deposition flux, exhibited substantial interannual variability, thereby exerting primary control over the temporal characteristics of total litterfall Hg deposition flux.

Environmental variables, including temperature, precipitation and wind speeds, generally exhibited weak correlations with the litterfall Hg and biomass deposition fluxes (Fig. 5f). However, a significant positive correlation was observed between growing-season precipitation and spruce tree litterfall Hg deposition flux, while no such relationship was found for pine trees. This may be attributed to the higher sensitivity of spruce stomatal conductance to water deficits (Lagergren and Lindroth, 2002). This regulates the exchange of GEM between the atmosphere and needles. Forest vegetation type may therefore influence the climate sensitivity of site-specific temporal patterns in the litterfall Hg deposition of boreal forests. In addition, extreme climate conditions, such as drought or excessive precipitation, can alter seasonal and annual litterfall biomass deposition in boreal forest (Frisko et al., 2024), and therefore potentially affect litterfall Hg deposition. Future studies should explore these interactions under changing climate conditions.

4. Conclusions and implications

In this study, we analyzed the Hg concentrations and deposition of individual litterfall components (needles, cones, twigs, and othermaterial) in a boreal forest in northern Sweden from 1987 to 2000. Our results show that pine and spruce needle Hg concentrations exhibited a general decadal decline (22 %-26 %) over 14 years, tracking the 41 % reduction in atmospheric GEM. In contrast, non-foliar litter component Hg concentrations (twigs, cones, and other-material) showed no significant trend. Importantly, total litterfall Hg deposition fluxes remained stable (11.7 \pm 1.8 $\mu g\,m^{-2}\,yr^{-1}),$ indicating that decadal atmospheric GEM declines did not translate into reduced ecosystem Hg inputs to the soil via litterfall. The individual component contributions of needles, cones, twigs, and other-material litter to the annual total litterfall Hg deposition fluxes were 44 \pm 8.7 %, 2 \pm 1.2 %, 32 \pm 9.0 %, and 22 \pm 8.8 %, respectively. Non-foliar litter, contributing 55 % of total Hg deposition despite lower biomass, played a dominant role in Hg cycling via litterfall. This underscores the influence of biological factors, such as litter composition and tree productivity, on Hg deposition in boreal forests. These findings have important implications for

evaluating the environmental effectiveness of the *Minamata Convention* on *Mercury*. The observed stability in litterfall Hg deposition, despite significant atmospheric Hg reductions, suggests potential lags in ecosystem deposition recovery and underscores the need to integrate biological pathways into monitoring frameworks. We recommend that future assessments of Hg deposition trends include long-term monitoring of individual litter components, especially non-foliar litter, to more accurately track ecosystem responses to emission controls under changing climate conditions.

CRediT authorship contribution statement

Xiangwen Zhang: Writing – original draft, Methodology, Investigation, Data curation. Haijun Peng: Writing – original draft, Visualization, Software, Formal analysis, Conceptualization. Stefan Osterwalder: Writing – review & editing, Methodology, Formal analysis. Kevin Bishop: Writing – review & editing, Methodology, Formal analysis, Conceptualization. Mats B. Nilsson: Methodology, Conceptualization. Matthias Peichl: Writing – review & editing, Methodology, Data curation. Erik Björn: Writing – review & editing, Resources, Formal analysis. Wei Zhu: Writing – review & editing, Supervision, Project administration, Methodology, Funding acquisition, Formal analysis, Conceptualization.

Declaration of competing interest

The authors declare that they have no known competing financial interests or personal relationships that could have appeared to influence the work reported in this paper.

Acknowledgements

This research was funded by the Swedish Research Council Vetenskapsrådet (2019–03709) and Formas (2021-00517), the Kempestiftelserna (SMK21-0057 and JCSMK24-610), and the SLU Quicksilver Infrastructure Platform. We thank Ulla Nylander and staff from the Vindeln Experimental Forests for performing the long-term collection and handling of the litter samples. Support was also supplied by the ICOS and SITES research infrastructures at Svartberget in the form of environmental monitoring data.

Appendix A. Supplementary data

Supplementary data to this article can be found online at https://doi.org/10.1016/j.envpol.2025.126901.

Data availability

Data will be made available on request.

References

- Arnold, J., Gustin, M.S., Weisberg, P.J., 2018. Evidence for nonstomatal uptake of Hg by aspen and translocation of Hg from foliage to tree rings in Austrian pine. Environ. Sci. Technol. 52, 1174–1182.
- Assad, M., Parelle, J., Cazaux, D., Gimbert, F., Chalot, M., Tatin-Froux, F., 2016. Mercury uptake into poplar leaves. Chemosphere 146, 1–7.
- Barquero, J.I., Rojas, S., Esbrí, J.M., García-Noguero, E.M., Higueras, P., 2019. Factors influencing mercury uptake by leaves of stone pine (Pinus pinea L.) in Almadén (Central Spain). Environ. Sci. Pollut. Res. 26, 3129–3137.
- Bishop, K., Shanley, J.B., Riscassi, A., de Wit, H.A., Eklöf, K., Meng, B., Mitchell, C., Osterwalder, S., Schuster, P.F., Webster, J., Zhu, W., 2020. Recent advances in understanding and measurement of mercury in the environment: terrestrial Hg cycling. Sci. Total Environ. 721, 137647.
- Blackwell, B., Driscoll, C., Maxwell, J., Holsen, T., 2014. Changing climate alters inputs and pathways of mercury deposition to forested ecosystems. Biogeochemistry 119, 215–228.
- Bradshaw, C.J., Warkentin, I.G., 2015. Global estimates of boreal forest carbon stocks and flux. Global Planet. Change 128, 24–30.

- Chen, C., Huang, J.-H., Li, K., Osterwalder, S., Yang, C., Waldner, P., Zhang, H., Fu, X., Feng, X., 2023. Isotopic characterization of Mercury atmosphere–foliage and atmosphere–soil exchange in a Swiss subalpine coniferous forest. Environ. Sci. Technol. 57, 15892–15903.
- Chi, J., Nilsson, M.B., Laudon, H., Lindroth, A., Wallerman, J., Fransson, J.E.S., Kljun, N., Lundmark, T., Ottosson Löfvenius, M., Peichl, M., 2020. The net landscape carbon balance—integrating terrestrial and aquatic carbon fluxes in a managed boreal forest landscape in Sweden. Glob. Change Biol. 26, 2353–2367.
- Chiarantini, L., Rimondi, V., Benvenuti, M., Beutel, M.W., Costagliola, P., Gonnelli, C., Lattanzi, P., Paolieri, M., 2016. Black pine (Pinus nigra) barks as biomonitors of airborne mercury pollution. Sci. Total Environ. 569–570, 105–113.
- Enrico, M., Le Roux, G., Heimbürger, L.-E., Van Beek, P., Souhaut, M., Chmeleff, J., Sonke, J.E., 2017. Holocene atmospheric mercury levels reconstructed from peat bog mercury stable isotopes. Environ. Sci. Technol. 51, 5899–5906.
- Faïn, X., Ferrari, C.P., Dommergue, A., Albert, M.R., Battle, M., Severinghaus, J., Arnaud, L., Barnola, J.M., Cairns, W., Barbante, C., 2009. Polar firn air reveals largescale impact of anthropogenic Mercury emissions during the 1970s. Proc. Natl. Acad. Sci. 106, 16114–16119.
- Frisko, R., Duchesne, L., Thiffault, E., Houle, D., Ouimet, R., 2024. Interannual variability and seasonality of litterfall in three temperate and boreal forest ecosystems of eastern Canada: a synthesis of long-term monitoring. For. Ecol. Manag. 568, 122069.
- Fu, X., Zhu, W., Zhang, H., Sommar, J., Yu, B., Yang, X., Wang, X., Lin, C.J., Feng, X., 2016. Depletion of atmospheric gaseous elemental mercury by plant uptake at mt. Changbai, Northeast China. Atmos. Chem. Phys. 16, 12861–12873.
- Gauthier, S., Bernier, P., Kuuluvainen, T., Shvidenko, A.Z., Schepaschenko, D.G., 2015. Boreal forest health and global change. Science 349, 819–822.
- Gerson, J.R., Driscoll, C.T., 2016. Is mercury in a remote forested watershed of the adirondack Mountains responding to recent decreases in emissions? Environ. Sci. Technol. 50, 10943–10950.
- Grangeon, S., Guedron, S., Asta, J., Sarret, G., Charlet, L., 2012. Lichen and soil as indicators of an atmospheric mercury contamination in the vicinity of a chlor-alkali plant (Grenoble, France). Ecol. Indic. 13, 178–183.
- Gustin, M.S., Dunham-Cheatham, S.M., Harper, J.F., Choi, W.-G., Blum, J.D., Johnson, M.W., 2022. Investigation of the biochemical controls on mercury uptake and mobility in trees. Sci. Total Environ. 851, 158101.
- Gustin, M.S., Gay, D.A., Choma, N., 2025. Assessment of recent mercury trends associated with the national atmospheric deposition program mercury litterfall network. Atmos. Environ. 347, 121097.
- Horowitz, H.M., Jacob, D.J., Amos, H.M., Streets, D.G., Sunderland, E.M., 2014.
 Historical mercury releases from commercial products: global environmental implications. Environ. Sci. Technol. 48, 10242–10250
- Horowitz, H.M., Jacob, D.J., Zhang, Y., Dibble, T.S., Slemr, F., Amos, H.M., Schmidt, J. A., Corbitt, E.S., Marais, E.A., Sunderland, E.M., 2017. A new mechanism for atmospheric mercury redox chemistry: implications for the global mercury budget. Atmos. Chem. Phys. 17, 6353–6371.
- Huang, J.-H., Berg, B., Chen, C., Thimonier, A., Schmitt, M., Osterwalder, S., Alewell, C., Rinklebe, J., Feng, X., 2023. Predominant contributions through lichen and fine litter to litterfall mercury deposition in a subalpine forest. Environ. Res. 229, 116005
- Jiskra, M., Wiederhold, J.G., Skyllberg, U., Kronberg, R.-M., Hajdas, I., Kretzschmar, R., 2015. Mercury deposition and Re-emission pathways in boreal forest soils investigated with Hg isotope signatures. Environ. Sci. Technol. 49, 7188–7196.
- Lagergren, F., Lindroth, A., 2002. Transpiration response to soil moisture in pine and spruce trees in Sweden. Agric. For. Meteorol. 112, 67–85.
- Laudon, H., Taberman, I., Ågren, A., Futter, M., Ottosson-Löfvenius, M., Bishop, K., 2013. The krycklan catchment study—A flagship infrastructure for hydrology, biogeochemistry, and climate research in the boreal landscape. Water Resour. Res. 49, 7154-7158.
- Lee, Y.H., Bishop, K.H., Munthe, J., 2000. Do concepts about catchment cycling of methylmercury and mercury in boreal catchments stand the test of time? Six years of atmospheric inputs and runoff export at Svartberget, northern Sweden. Sci. Total Environ. 260, 11–20.
- Li, C., Jiskra, M., Nilsson, M.B., Osterwalder, S., Zhu, W., Mauquoy, D., Skyllberg, U., Enrico, M., Peng, H., Song, Y., Björn, E., Bishop, K., 2023. Mercury deposition and redox transformation processes in peatland constrained by mercury stable isotopes. Nat. Commun. 14, 7389.
- Liu, Y., Liu, G., Wang, Z., Guo, Y., Yin, Y., Zhang, X., Cai, Y., Jiang, G., 2021. Understanding foliar accumulation of atmospheric Hg in terrestrial vegetation: progress and challenges. Crit. Rev. Environ. Sci. Technol. 1–22.
- Matin, G., Kargar, N., Buyukisik, H.B., 2016. Bio-monitoring of cadmium, lead, arsenic and mercury in industrial districts of Izmir, Turkey by using honey bees, propolis and pine tree leaves. Ecol. Eng. 90, 331–335.
- McLagan, D.S., Biester, H., Navrátil, T., Kraemer, S.M., Schwab, L., 2022. Internal tree cycling and atmospheric archiving of mercury: examination with concentration and stable isotope analyses. Biogeosciences 19, 4415–4429.
- Méndez-López, M., Parente-Sendín, A., Calvo-Portela, N., Gómez-Armesto, A., Eimil-Fraga, C., Alonso-Vega, F., Arias-Estévez, M., Nóvoa-Muñoz, J.C., 2023. Mercury in a birch forest in SW Europe: deposition flux by litterfall and pools in aboveground tree biomass and soils. Sci. Total Environ. 856, 158937.
- Muukkonen, P., Lehtonen, A., 2004. Needle and branch biomass turnover rates of Norway spruce (Picea abies). Can. J. For. Res. 34, 2517–2527.
- Navrátil, T., Nováková, T., Roll, M., Shanley, J.B., Kopáček, J., Rohovec, J., Kaňa, J., Cudlín, P., 2019. Decreasing litterfall mercury deposition in central European coniferous forests and effects of bark beetle infestation. Sci. Total Environ. 682, 213–225.

- Navrátil, T., Nováková, T., Shanley, J.B., Rohovec, J., Matoušková, Š., Vaňková, M., Norton, S.A., 2018. Larch tree rings as a tool for reconstructing 20th century central European atmospheric mercury trends. Environ. Sci. Technol. 52, 11060–11068.
- Navrátil, T., Rohovec, J., Nováková, T., Roll, M., Cudlín, P., Oulehle, F., 2024. Quarter century of mercury litterfall at a coniferous forest responding to climate change, Central Europe. Environ. Sci. Pollut. Control Ser. 31, 34936–34952.
- Navrátil, T., Rohovec, J., Shanley, J.B., Matoušková, Š., Roll, M., Nováková, T., Krám, P., Tesař, M., Myška, O., Oulehle, F., 2025. Mercury cycling in the Czech GEOMON network catchments recovering from acid deposition and facing climate change. Biogeochemistry 168, 45.
- Noumonvi, K.D., Ågren, A.M., Ratcliffe, J.L., Öquist, M.G., Ericson, L., Tong, C.H.M., Järveoja, J., Zhu, W., Osterwalder, S., Peng, H., Erefur, C., Bishop, K., Laudon, H., Nilsson, M.B., Peichl, M., 2023. The Kulbäcksliden Research infrastructure: a unique setting for northern peatland studies. Front. Earth Sci. 11, 1194749.
- Obrist, D., Kirk, J.L., Zhang, L., Sunderland, E.M., Jiskra, M., Selin, N.E., 2018. A review of global environmental mercury processes in response to human and natural perturbations: changes of emissions, climate, and land use. Ambio 47, 116–140.
- Obrist, D., Roy, E.M., Harrison, J.L., Kwong, C.F., Munger, J.W., Moosmüller, H., Romero, C.D., Sun, S., Zhou, J., Commane, R., 2021. Previously unaccounted atmospheric mercury deposition in a midlatitude deciduous forest. Proc. Natl. Acad. Sci. 118, e2105477118.
- Outridge, P.M., Mason, R.P., Wang, F., Guerrero, S., Heimbürger-Boavida, L.E., 2018. Updated global and Oceanic mercury budgets for the United Nations global mercury assessment 2018. Environ. Sci. Technol. 52, 11466–11477.
- Peckham, M.A., Gustin, M.S., Weisberg, P.J., 2019. Assessment of the suitability of tree rings as archives of global and regional atmospheric mercury pollution. Environ. Sci. Technol. 53, 3663–3671.
- Peichl, M., Martínez-García, E., Fransson, J.E., Wallerman, J., Laudon, H., Lundmark, T., Nilsson, M.B., 2023. Landscape-variability of the carbon balance across managed boreal forests. Glob. Change Biol. 29, 1119–1132.
- Peng, H., Zhang, X., Bishop, K., Marshall, J., Nilsson, M.B., Li, C., Björn, E., Zhu, W., 2024. Tree rings mercury controlled by atmospheric gaseous elemental mercury and tree physiology. Environ. Sci. Technol. 58, 16833–16842.
- Reich, P.B., Oleksyn, J., Modrzynski, J., Tjoelker, M.G., 1996. Evidence that longer needle retention of spruce and pine populations at high elevations and high latitudes is largely a phenotypic response. Tree Physiol. 16, 643–647.
- Reich, P.B., Rich, R.L., Lu, X., Wang, Y.-P., Oleksyn, J., 2014. Biogeographic variation in evergreen conifer needle longevity and impacts on boreal forest carbon cycle projections. Proc. Natl. Acad. Sci. 111, 13703–13708.
- Risch, M.R., DeWild, J.F., Gay, D.A., Zhang, L., Boyer, E.W., Krabbenhoft, D.P., 2017.
 Atmospheric mercury deposition to forests in the eastern USA. Environ. Pollut. 228, 8–18
- Roos-Barraclough, F., Martinez-Cortizas, A., García-Rodeja, E., Shotyk, W., 2002. A 14 500 year record of the accumulation of atmospheric mercury in peat: volcanic signals, anthropogenic influences and a correlation to bromine accumulation. Earth Planet Sci. Lett. 202. 435–451.
- Rydberg, J., Gälman, V., Renberg, I., Bindler, R., Lambertsson, L., Martínez-Cortizas, A., 2008. Assessing the stability of Mercury and methylmercury in a varved Lake sediment deposit. Environ. Sci. Technol. 42, 4391–4396.
- Selin, H., Selin, N.E., 2022. From Stockholm to Minamata and beyond: governing mercury pollution for a more sustainable future. One Earth 5, 1109–1125

- Selin, N.E., 2009. Global biogeochemical cycling of mercury: a review. Annu. Rev. Environ. Resour. 34, 43–63.
- Siwik, E.I., Campbell, L.M., Mierle, G., 2009. Fine-scale mercury trends in temperate deciduous tree leaves from Ontario, Canada. Sci. Total Environ. 407, 6275–6279.
- Stamenkovic, J., Gustin, M.S., 2009. Nonstomatal versus stomatal uptake of atmospheric mercury. Environ. Sci. Technol. 43, 1367–1372.
- Tang, J.-W., Cao, M., Zhang, J.-H., Li, M.-H., 2010. Litterfall production, decomposition and nutrient use efficiency varies with tropical forest types in Xishuangbanna, SW China: a 10-year study. Plant Soil 335, 271–288.
- Tørseth, K., Aas, W., Breivik, K., Fjæraa, A.M., Fiebig, M., Hjellbrekke, A.G., Lund Myhre, C., Solberg, S., Yttri, K.E., 2012. Introduction to the European monitoring and evaluation programme (EMEP) and observed atmospheric composition change during 1972–2009. Atmos. Chem. Phys. 12, 5447–5481.
- Vanhala, P., Bergström, I., Haaspuro, T., Kortelainen, P., Holmberg, M., Forsius, M., 2016. Boreal forests can have a remarkable role in reducing greenhouse gas emissions locally: land use-related and anthropogenic greenhouse gas emissions and sinks at the municipal level. Sci. Total Environ. 557, 51–57.
- Wang, X., Bao, Z., Lin, C.-J., Yuan, W., Feng, X., 2016. Assessment of global mercury deposition through litterfall. Environ. Sci. Technol. 50, 8548–8557.
- Wang, X., Yuan, W., Lin, C.-J., Feng, X., 2021. Mercury cycling and isotopic fractionation in global forests. Crit. Rev. Environ. Sci. Technol. 52, 3763–3786.
- Wohlgemuth, L., Osterwalder, S., Joseph, C., Kahmen, A., Hoch, G., Alewell, C., Jiskra, M., 2020. A bottom-up quantification of foliar mercury uptake fluxes across Europe. Biogeosciences 17, 6441–6456.
- Wohlgemuth, L., Rautio, P., Ahrends, B., Russ, A., Vesterdal, L., Waldner, P., Timmermann, V., Eickenscheidt, N., Fürst, A., Greve, M., Roskams, P., Thimonier, A., Nicolas, M., Kowalska, A., Ingerslev, M., Merilä, P., Benham, S., Iacoban, C., Hoch, G., Alewell, C., Jiskra, M., 2022. Physiological and climate controls on foliar mercury uptake by European tree species. Biogeosciences 19, 1335–1353.
- Wright, L.P., Zhang, L., Marsik, F.J., 2016. Overview of mercury dry deposition, litterfall, and throughfall studies. Atmos. Chem. Phys. 16, 13399–13416.
- Xu, Z., Wang, Z., Zhang, X., 2022. Mapping the forest litterfall mercury deposition in China. Sci. Total Environ. 839, 156288.
- Yang, Y., Yanai, R.D., Driscoll, C.T., Montesdeoca, M., Smith, K.T., 2018. Concentrations and content of mercury in bark, wood, and leaves in hardwoods and conifers in four forested sites in the northeastern USA. PLoS One 13, e0196293.
- Yuan, W., Wang, X., Lin, C.-J., Song, Q., Zhang, H., Wu, F., Liu, N., Lu, H., Feng, X., 2023. Deposition and Re-Emission of Atmospheric elemental mercury over the tropical Forest floor. Environ. Sci. Technol. 57, 10686–10695.
- Zhang, Y., Jacob, D.J., Horowitz, H.M., Chen, L., Amos, H.M., Krabbenhoft, D.P., Slemr, F., St Louis, V.L., Sunderland, E.M., 2016. Observed decrease in atmospheric mercury explained by global decline in anthropogenic emissions. Proc. Natl. Acad. Sci. 113, 526–531.
- Zhou, J., Bollen, S.W., Roy, E.M., Hollinger, D.Y., Wang, T., Lee, J.T., Obrist, D., 2023. Comparing ecosystem gaseous elemental mercury fluxes over a deciduous and coniferous forest. Nat. Commun. 14, 2722.
- Zhou, J., Obrist, D., Dastoor, A., Jiskra, M., Ryjkov, A., 2021. Vegetation uptake of mercury and impacts on global cycling. Nat. Rev. Earth Environ. 2, 269–684.
- Zhu, W., Lin, C.J., Wang, X., Sommar, J., Fu, X., Feng, X., 2016. Global observations and modeling of atmosphere-surface exchange of elemental mercury: a critical review. Atmos. Chem. Phys. 16, 4451–4480.